

## Foaming Technique of Porous Aluminum/Intermetallics Composites by Precursor Method

Makoto Kobashi<sup>1</sup>, Naoyuki Kanetake<sup>1</sup>

<sup>1</sup>Department of Materials Science and Engineering, Nagoya University, 1 Furo-cho, Chikusa-ku, Nagoya 464-8603, Japan

The authors have developed a novel fabrication process for porous aluminum/intermetallics composites using combustion reactions. In this technique, the reaction between (i) aluminum and nickel and (ii) aluminum and titanium was used. An exothermic agent powder, which releases high heat of reaction, was additionally used to control porosity. The elemental powders and exothermic agent were blended and compacted to make a precursor. When the precursor was heated, the combustion reaction occurred and the precursor expanded due to a gas evaporation (mainly hydrogen), which was originally adsorbed at or absorbed in the elemental powders. The pore morphology was affected mainly by (i) elemental powder blending ratio, (ii) additive amount of exothermic agent, (iii) elemental powder size and (iv) relative density of the precursor. The adequate blending ratios of Al/Ni and Al/Ti to obtain sufficiently foamed specimens were identified. By adding 10vol% exothermic agent, the porosity of the specimen became higher than that of the non-added specimen. High porosity was achieved by using smaller nickel and titanium powders. Hot extrusion was effective to fabricate high porosity specimen than the cold compaction. By selecting the appropriate conditions, highly porous aluminum/intermetallics composites with homogeneous pore distribution were obtained.

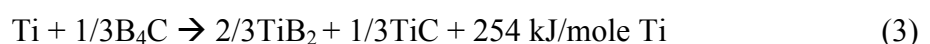
**Keywords:** Porous material, intermetallics foam, combustion reaction,  $Al_3Ni$ ,  $Al_3Ti$

### 1. Introduction

Porous metals exhibit various unique physical and mechanical properties, such as low apparent density and high strain energy absorbing capability [1-4]. Porous aluminum is one of the most enthusiastically investigated materials among wide variety of porous metals [5-10]. One reason is that effective blowing agents like  $TiH_2$ ,  $ZrH_2$  and  $CaCO_3$ , which decompose and release gaseous phase at around the melting point of aluminum or aluminum alloys are available [11-15]. If metals can be substituted by intermetallics or their composites, such porous materials can be used under extremely severe environments, e.g. thermal barrier coatings at high temperatures and heavy load-bearing components [16-18]. However, the melting points of intermetallics are generally higher than those of light metals, and it is more difficult and more energy consuming process to introduce pores inside intermetallics. The authors have developed a novel fabrication process for porous aluminum/intermetallics composites using combustion reaction (combustion foaming process). Combustion synthesis is one of the attractive processing routes for producing intermetallics and their composites because high-melting-point material can be produced with little energy and without special equipments [19,20]. Fig. 1 shows a brief outline of the combustion foaming process for the synthesis of porous aluminum/intermetallics composite. Fundamentally, the reactions between elemental powders shown below are used in this technique.



As shown in Fig. 1, boron carbide ( $B_4C$ ) powder is blended in the powder compacted precursor.  $B_4C$  powder reacts with titanium, and generates large amount of reaction heat as shown in the following equation.



This heat of reaction assists the progress of the  $\text{Al}_3\text{Ni}$  and  $\text{Al}_3\text{Ti}$  formation and is expected to enhance the foaming behavior. Therefore,  $\text{B}_4\text{C}$  and equivalent amount of titanium, which is required for Eq. 3, were used as the “exothermic agent” in this study. In the present paper, we discuss the effects of several processing parameters (elemental powder blending ratio, additive amount of exothermic agent, elemental powder size and relative density of the precursor) on pore morphology of porous aluminum/intermetallics composites.

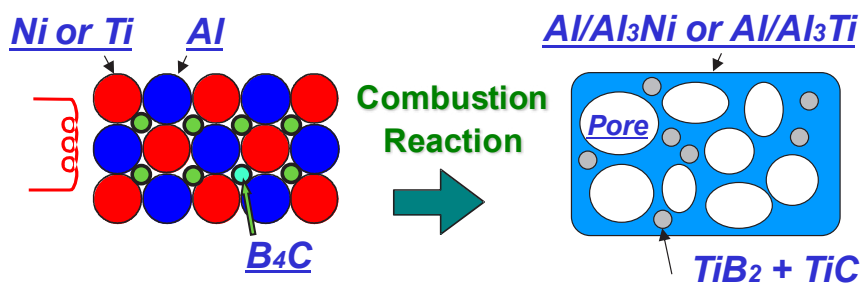


Fig. 1 Schematic illustration of combustion foaming process for  $\text{Al}/\text{Al}_3\text{Ni}$  and  $\text{Al}/\text{Al}_3\text{Ti}$  composite foam.

## 2. Experiment

### 2.1 Fabrication of porous aluminum/intermetallics composite

Aluminum ( $10\mu\text{m}$ ,  $<45\mu\text{m}$ ,  $106\sim 180\mu\text{m}$ , 99.99%), titanium ( $<45\mu\text{m}$ ,  $90\sim 150\mu\text{m}$ ,  $150\sim 250\mu\text{m}$ , 99.9%), nickel ( $3\sim 5\mu\text{m}$ ,  $<45\mu\text{m}$ ,  $<75\mu\text{m}$ , 99.9%) and  $\text{B}_4\text{C}$  (ave.  $10\mu\text{m}$ , 99%) powders were used as starting powders. In the following sections, aluminum powder with a diameter of  $45\mu\text{m}$ , for example, is denoted as Al(45). First of all, (i) aluminum and nickel or (ii) aluminum and titanium powders were blended by various molar ratios.  $\text{B}_4\text{C}$  powder and equivalent amount of titanium, spent for the reaction shown in Eq. 3, were additionally blended in the starting powder (exothermic agent). The amount of exothermic agent was defined by the volume fraction of ceramic particles ( $\text{TiC}$ ,  $\text{TiB}_2$ ) in the solid section, and the volume fraction was set from 0 to 15%. After all elemental powders were blended, the blended powder was compacted either by single-axis pressing at room temperature (30, 50, 100 and 165MPa) or by hot extrusion at  $400^\circ\text{C}$  (240MPa, extrusion ratio:7.1) to make cylindrical shape precursors ( $\phi=15\text{mm}$ ,  $h=15\text{mm}$ ). The precursor was inserted into a furnace filled with argon gas, and then heated to induce the combustion reaction. The apparent density of the porous specimen was measured by Archimedes method to calculate porosity.

### 2.2 Gas analysis

The specimen used for gas analysis was  $\text{Al}_3\text{Ni}$  foam (Al/Ni mole ratio: 3.0, exothermic agent: 0vol%). The porous specimens were drilled ( $\phi$  2mm) in a chamber, and the gas filled in the pores were extracted. Quantitative analysis of gas phase in the cells of intermetallics foam was carried out by a mass spectrometer.

## 3. Results and discussions

### 3.1 Characterization and pore formation mechanism of $\text{Al}/\text{Al}_3\text{Ni}$ foam

Fig. 2 shows the cross-section of Al-Ni combustion synthesized foam (Al/Ni mole ratio = 4.0, exothermic agent addition: 5.0vol%). The porosity was over 80% and the homogeneously dispersed pores of 3-4mm in diameter were observed. The cell wall thickness was below  $100\mu\text{m}$  and was consisting of aluminum and  $\text{Al}_3\text{Ni}$  intermetallics. This thin wall thickness could be achieved by the rapid heating and cooling profile of the combustion reaction. Fig. 3 shows the results of mass spectrum of the extracted gas from the pores of the specimens. The X and Y axis of Fig. 3 show mass number and the intensity of the mass spectrum, respectively. The integrated spectrum intensity was

calculated to derive the mass ratio of the gas phases, and the result is shown in Table 1. The major gas source was turned out to be hydrogen, which originally adsorbed at or absorbed in the elemental powders. The Ar gas detected in the cell was the residual gas in the porosity of the precursor, since the combustion foaming experiment was carried out in Ar gas atmosphere.

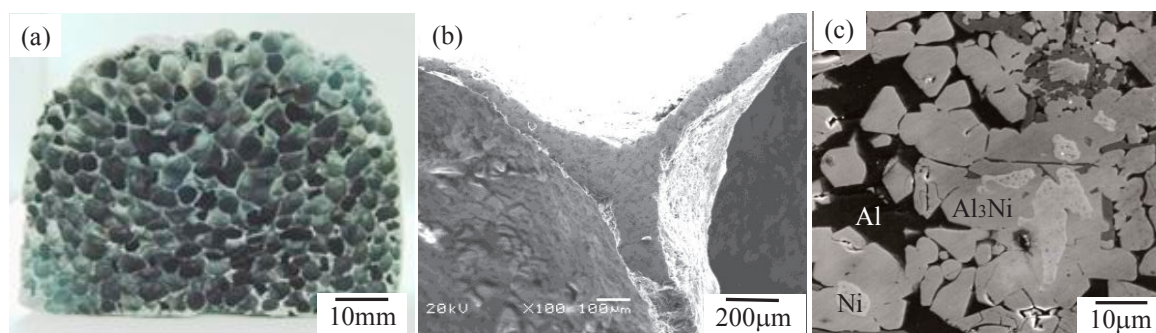


Fig. 2 Cross-section of the combustion synthesized foam (Al/Ni= 4.0, exothermic agent addition= 5.0vol%), (a) macroscopic cross-section, (b) cell wall structure and (c) microstructure of the cell.

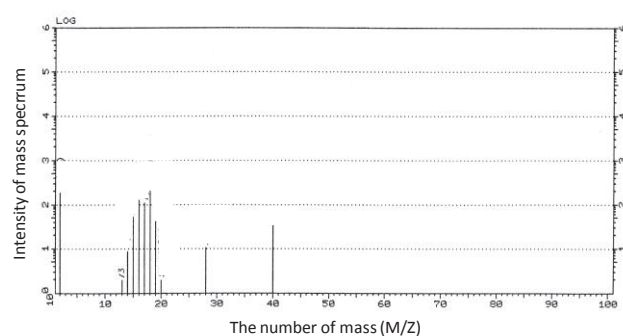


Fig. 3 The mass spectrum of gas phase extracted from the pores of  $\text{Al}_3\text{Ni}$  foam.

Table 1 Gas composition in the pores of  $\text{Al}_3\text{Ni}$  foam

Gas	Mass %
<b>H<sub>2</sub></b>	<b>68.7</b>
<b>CH<sub>4</sub></b>	<b>19.6</b>
<b>N<sub>2</sub>,CO</b>	<b>3.0</b>
<b>Ar</b>	<b>8.7</b>
<b>Total</b>	<b>100</b>

### 3.2 Effect of blending ratio of elemental powders on cell morphology

Fig. 4 shows cross-sections of specimens (Al/Ni and Al/Ti mole ratio: 4.0) fabricated by adding various amounts of exothermic agent (0, 5, 10, 15vol%). The porosity was apparently increased with an addition of the exothermic agent by 10vol%. This is because the high heat of reaction of  $\text{TiB}_2$  and  $\text{TiC}$  formation assisted the progress of the  $\text{Al}_3\text{Ni}$  and  $\text{Al}_3\text{Ti}$  formation. Furthermore, dispersion of fine ceramic particles was reported to be effective for maintaining the stable foam structure [21-24], and may be beneficial to this specimen as well. However, an overdose of exothermic agent showed a negative effect on the pore formation because of the extremely high viscosity. Fig. 5 shows cross-sections of specimens fabricated by various Al/Ni and Al/Ti mole ratios (Al/Ni, Al/Ti mole ratio: 4.0~8.0). With respect to Al-Ti specimens, high porosity was maintained within wide range of Al/Ti ratios. As for Al-Ni specimen, combustion reaction did not occur by increasing Al/Ni ratio (>7.0). Sufficient amount of molten phase was essential to obtain highly porous specimens. Since the combustion temperature of this specimen was higher than the melting point of aluminum and almost the same level of intermetallics ( $\text{Al}_3\text{Ti}$ ,  $\text{Al}_3\text{Ni}$ ), most of the molten phase during the combustion period might be aluminum. However, the excess amount of aluminum absorbed the reaction heat, and played a negative effect on the porosity, especially for Al-Ni specimens.

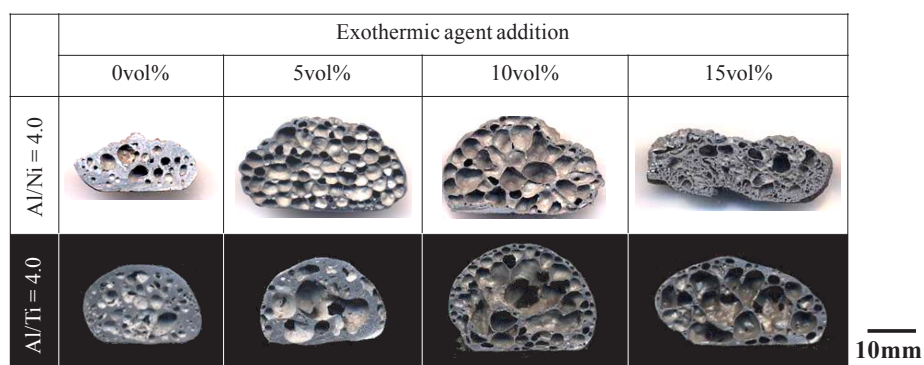


Fig. 4 Cross-sections of specimens fabricated by adding various amounts of exothermic agent (0, 5, 10, 15vol%).

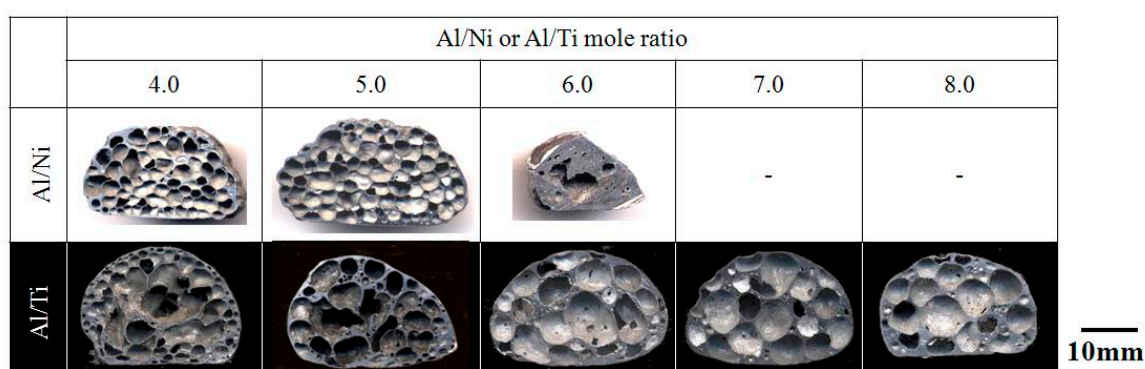


Fig. 5 Cross-sections of Al-Ni (exothermic agent: 5vol%) and Al-Ti (exothermic agent: 10vol%) specimens fabricated by various mole ratios.

### 3.3 Effect of elemental powder size on the combustion behavior and pore formation

Fig. 6 shows the temperature profile of the specimens made from elemental powders with various sizes (Al/Ni=4.0, Exothermic agent= 5.0vol%). A slight increase in the maximum combustion temperature was observed by increasing aluminum powder size due to an increase in the relative density of the precursor. A significant decrease was observed by increasing the nickel size. It is well-known that nickel powder size is a crucial factor which determines the intensity of the exothermic reaction between nickel and aluminum [25]. This is because the diffusion of molten aluminum into nickel occurs during the combustion reaction. Table 2 shows porosity of the specimens made from elemental powders with various sizes. Relatively higher porosity was obtained by using the smaller nickel and titanium powders.

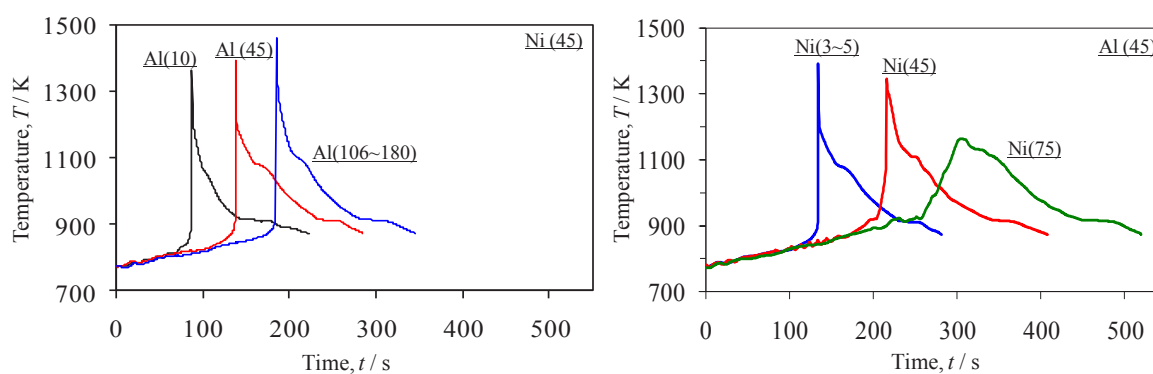


Fig. 6 Temperature profile of the specimens made from elemental powders with various sizes.

Table 2 Porosity of the specimens made from elemental powders with various sizes.

Element	Ni			Ti		
	3~5	<45	<75	<45	90~150	150~250
Al(10)	70%	59%	49%	79%	78%	76%
Al(45)	78%	72%	63%	74%	72%	55%
Al(106~180)	82%	73%	52%	69%	69%	59%

### 3.4 Compacting pressure effect on the cell morphology

Fig. 7 shows the porosity of the porous specimens as a function of relative density of the precursors. Precursors with relative density of 0.95 were prepared by a hot extrusion. Other precursors were prepared by single-axis pressing at room temperature. The highest porosity was achieved when the precursor was fabricated by hot extrusion for both Al-Ti and Al-Ni specimens. The reason for the high porosity of the hot-extruded precursor may be high relative density and firmly bonded elemental powders, which prevented the dissipation of gas phase to the ambient atmosphere.

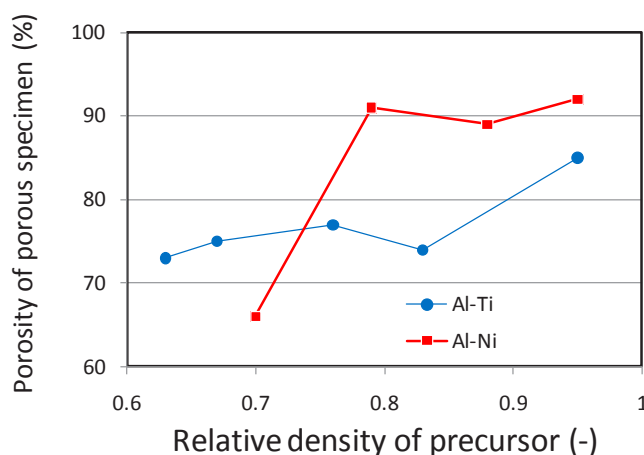


Fig. 7 Porosity of porous specimens as a function of relative density of Al-Ti and Al-Ni precursors.

## 4. Conclusion

Porous Al/Al<sub>3</sub>Ni and Al/Al<sub>3</sub>Ti composites were fabricated by a reactive powder processing technology (combustion foaming process). Effects of processing parameters ((i) elemental powder blending ratio, (ii) addition of exothermic agent, (iii) elemental powder size and (iv) relative density of the precursor) on porosity and pore morphology were investigated and the following results were obtained.

1. The porosity of the porous specimen (Al/Ni=4.0, exothermic agent=5.0vol%) was over 80% and the homogeneously dispersed pores of 3-4 mm diameter were observed. The cell wall thickness was below 100 $\mu$ m and was consisting of aluminum and Al<sub>3</sub>Ni intermetallics.
2. The major gas source was hydrogen, which was originally adsorbed at or absorbed in the elemental powders.
3. The porosity was apparently increased with an addition of the exothermic agent by 10vol%. However, an overdose of exothermic agent showed a negative effect on the pore formation because of the extremely high viscosity.

4. By increasing the aluminum blending ratio in the precursor, the porous specimen could not be obtained for Al-Ni specimens. The excess amount of aluminum absorbed the reaction heat, and played a negative effect on the porosity.
5. A slight increase in the maximum combustion temperature was observed by increasing aluminum powder size. However, a significant decrease was observed by increasing the nickel size. The porosity of the specimen decreased by increasing Ni powder size.
6. Hot extrusion was effective to fabricate high porosity specimen than the cold compaction.

### Acknowledgement

This study was supported by Industrial Technology Research Grant Program in 2008 from New Energy and Industrial Technology Development Organization (NEDO) of Japan.

### References

- [1] J. Baumeister, J. Banhart and M. Weber: *Mater. Design* 18 (1997) 217-220.
- [2] L. Ma and Z. Song: *Scr. Mater.* 39 (1998) 1523-1528.
- [3] J. Banhart: *Prog. Mater. Sci.* 46 (2001) 559-632.
- [4] J. Banhart and J. Baumeister: *J. Mater. Sci.* 33 (1998) 1431-1440.
- [5] Y. Chino, H. Nakanishi, M. Kobata, H. Iwasaki and M. Mabuchi: *Scr. Mater.* 47 (2002) 769-773.
- [6] I. Duarte and J. Banhart: *Acta Mater.* 48 (2000) 2349-2362.
- [7] S. Asavavisithchai and A.R. Kennedy: *Adv. Eng. Mater.* 8 (2006) 810-815.
- [8] L. Bonaccorsi and E. Proverbio: *Adv. Eng. Mater.* 8 (2006) 864-869.
- [9] B. Matijasevic and J. Banhart: *Scr. Mater.* 54 (2006) 503- 508.
- [10] V. Gergely and T.W. Clyne: *Acta Mater.* 52 (2004) 3047-3058.
- [11] A.R. Kennedy and V.H. Lopez: *Mater. Sci. Eng. A357* (2003) 258-263.
- [12] A.R. Kennedy: *Scr. Mater.* 47 (2002) 763-767.
- [13] B. Matijasevic-Lux, J. Banhart, S. Fiechter, O. Gorke and N. Wanderka: *Acta Mater.* 54 (2006) 1887-1900.
- [14] L.E.G. Cambronero, J.M. Ruiz-Roman, F.A. Corpas and J.M. Ruiz Prieto: *J. Mat. Proc. Tech.* 209 (2009) 1803-1809.
- [15] F. von Zeppelin, M. Hirscher, H. Stanzick and J. Banhart: *Compos. Sci. Tech.*, 63 (2003) 2293-2300.
- [16] A.M. Hodge and D.C. Dunand: *Intermetallics* 9 (2001) 581-589.
- [17] R. Darolia, *Intermetallics* 8 (2000) 1321-1327.
- [18] Y. Zhao, M. Taya, Y. Kang and A. Kawasaki: *Acta Mater.* 53 (2005) 337-343.
- [19] S.H. Lee, J.H. Lee, Y.H. Lee, D.H. Shin and Y.S. Kim: *Mater. Sci. Eng. A281* (2000) 275-285.
- [20] M.C. Dumez, R.M. Marin-Ayral and J.C. Tedenac: *J. Alloy. Compd.* 268 (1998) 141-151.
- [21] V. Gergely and T.W. Clyne: *Acta Mater.* 52 (2004) 3047-3058.
- [22] W. Deqing and S. Ziyuan: *Mater. Sci. Eng. A361* (2003) 45-49.
- [23] T. Wubben, H. Stanzick, J. Banhart and S. Odenbach: *J. Phys. Condens. Matter* 15 (2003) S427-S433.
- [24] J. Banhart: *Europhysics News* Jan./Feb. (1999) 17-20.
- [25] A. Hibino, S. Matsuoka and M. Kiuchi: *J. Mater. Proc. Tech.* 112 (2001) 127-135.